

## [Supplementary Information]

### **Controlled synthesis and characterization of the enhanced local field of octahedral Au nanocrystals**

Jinhwa Heo,<sup>†,‡</sup> Deok-Soo Kim,<sup>§</sup> Zee Hwan Kim,<sup>\*,§</sup> Young Wook Lee,<sup>†</sup> Dongheun Kim,<sup>†</sup> Minjung Kim,<sup>†</sup> Kihyun Kwon,<sup>†</sup> Hyung Ju Park,<sup>‡</sup> Wan Soo Yun,<sup>\*,‡</sup> and Sang Woo Han<sup>\*,†</sup>

*Department of Chemistry, Research Institute of Natural Science, Environmental Biotechnology National Core Research Center, Gyeongsang National University, Jinju 660-701, Korea, Division of Advanced Technology, Korea Research Institute of Standards and Science, Daejeon 305-600, Korea, and Department of Chemistry, Korea University, Seoul 136-701, Korea*

\*Corresponding author. *E-mail:* swhan@gnu.ac.kr; zhkim@korea.ac.kr;  
wsyun@kriss.re.kr

---

<sup>†</sup> Gyeongsang National University.

<sup>‡</sup> Korea Research Institute of Standards and Science.

<sup>§</sup> Korea University.

## Experimental

**Synthesis of octahedral Au nanoparticles.** In a typical synthesis of octahedral gold nanoparticles, a 20 mL aqueous solution of  $\text{HAuCl}_4$  ( $1.25 \times 10^{-4}$  M, 99.9+%, Aldrich) and cetyltrimethylammonium bromide (CTAB) (10 mM, 95%, Aldrich) was prepared. To this solution, an aqueous solution of L-ascorbic acid (100 mM, 100  $\mu\text{L}$ , 99.0%, Sigma) was added. The light yellow color of the gold salt in the CTAB solution disappeared when ascorbic acid was added owing to the reduction of  $\text{Au}^{3+}$  to  $\text{Au}^+$ . To this mixture, an aqueous solution of NaOH (100 mM, 100  $\mu\text{L}$ ) was quickly injected to induce the particle formation. With gentle shaking, the color of the solution changed from pale-pink and finally to purple-red within 20 min. The temperature was maintained at 25 °C throughout the reaction. The gold nanoparticles were centrifuged (7,000 rpm) and redispersed in water three times to remove the excess reactants in the solution. Any organic precipitates and blurring of microscopy images that were usually observed in unpurified samples were not observed in the electron microscopy measurements of the purified samples. Moreover, the characteristic UV-vis spectral feature of gold hydrosol was maintained after the purification step, indicating that the dispersibility of nanoparticles was not affected by the washing/redispersing process.

**Characterization.** The extinction spectra were recorded with a UV-vis absorption spectrometer (SINCO S-3100). Scanning electron microscopy (SEM) images of the samples were taken with FEI field-emission scanning electron microscope (Sirion 400). Transmission electron microscopy (TEM) images were obtained with a JEOL JEM-2010 transmission electron microscope operating at 200 kV. High-resolution TEM (HRTEM) characterizations were performed with a FEI Technai G2 F30 Super-Twin transmission electron microscope operating at 300 kV. X-ray diffraction (XRD) patterns were obtained with a Bruker AXS D8 DISCOVER diffractometer using  $\text{Cu K}\alpha$  (0.1542 nm) radiation. Raman spectra were obtained using a Jobin Yvon/HORIBA Lab RAM spectrometer with the 632.8 nm radiation from an air-cooled He/Ne laser as the excitation source. The Raman band of a silicon wafer at 520  $\text{cm}^{-1}$  was used to calibrate the spectrometer. A glass capillary with an outer diameter of 1.3-1.8 mm was used as a sampling device. The Raman scattering enhancement factors ( $EF$ ) were calculated by using the following relationship:  $EF =$

$(I_{\text{SERS}}/I_{\text{Raman}})/(C_{\text{SERS}}/C_{\text{Raman}})$  (Ref.: Kwon, K.; Lee, K. Y.; Lee, Y. W.; Kim, M.; Heo, J.; Ahn, S. J.; Han, S. W. *J. Phys. Chem. C* **2007**, *111*, 1161.), where  $I_{\text{SERS}}$  and  $I_{\text{Raman}}$  are the measured intensity of the selected peak of analyte molecule in the SERS and the normal Raman spectra of the aqueous solution, respectively, and  $C_{\text{SERS}}$  and  $C_{\text{Raman}}$  are the concentration of analyte in the SERS sample and in the aqueous solution, respectively. The details of the scattering-type apertureless near-field scanning optical microscopy (ANSOM) instrument and its operating principles are already described elsewhere (Ref.: Kim, Z. H.; Liu, B.; Leone, S. R. *J. Phys. Chem. B* **2005**, *109*, 8503; Kim, Z. H.; Ahn, S.-H.; Liu, B.; Leone, S. R. *Nano Lett.* **2007**, *7*, 2258; Kim, Z. H.; Leone, S. R. *Opt. Express* **2008**, *16*, 1733.). The PtIr coated atomic force microscopy (AFM) tip is dithered near the resonance frequency of the cantilever ( $\Omega \sim 300$  kHz) with full amplitude of 20-100 nm above the sample surface (Fig. S3). Linearly polarized (p-polarized with respect to the sample surface) light from a laser (HeNe, 632.8 nm) is focused onto the tip-sample junction with an angle of  $30^\circ$  with respect to the sample surface via an objective lens. Back-scattered light from the junction is collected by the same lens and homodyne-detected to give separate intensity and phase information of the scattered field. Throughout the current experiment, we detect only the p-polarization component of the scattered light using the quarter-wave plate (QWP) placed in reference arm of the interferometer. The far-field background signal that originates from scattering by the sample surface and tip shaft is removed by the third harmonic ( $3\Omega \sim 900$  kHz) demodulation technique via a lock-in amplifier. The optical and AFM topography images are simultaneously acquired by raster-scanning the sample and recording the optical and topographic signals. The Au nanooctahedra and nanosphere (nominal diameters of 100 nm) samples are prepared by drop-casting Au hydrosols onto silicon substrates.

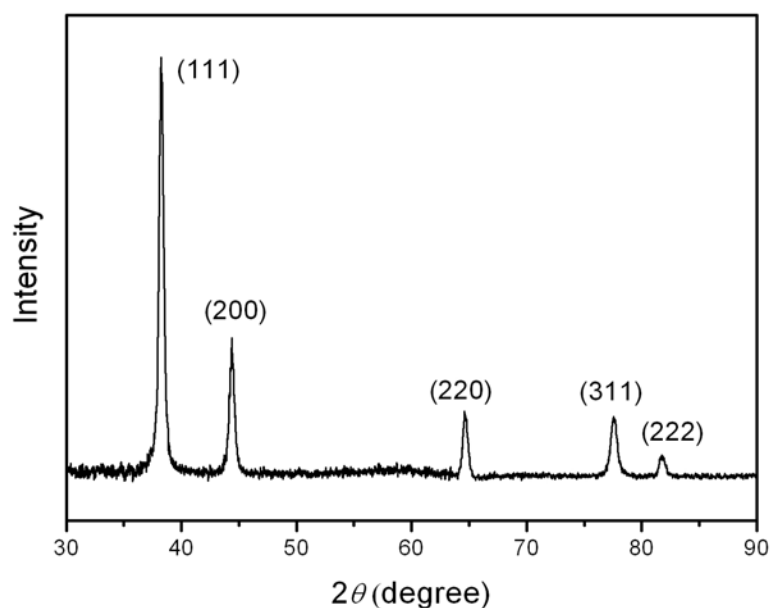


**Fig. S1.** XRD pattern of the octahedral Au nanoparticles. Four peaks observed at 38.2°, 44.4°, 64.7°, 77.6°, and 81.7° can be indexed to the (111), (200), (220), (311), and (222) reflections of face-centered cubic (fcc) structure of metallic Au, respectively (JCPDS, card no. 04-0784), showing the pure crystalline nature of the prepared particles. The intensity ratio between the (200) and the (111) diffractions ( $I_{(200)}/I_{(111)}$ ) of 0.32 for the prepared sample is much smaller than the conventional bulk intensity ratio ( $\sim 0.53$ ), indicating that the faces of these nanoparticles are primarily composed of {111} planes (Ref.: Kim, F.; Connor, S.; Song, H.; Kuykendall, T.; Yang, P. *Angew. Chem. Int. Ed.* **2004**, 43, 3673.).

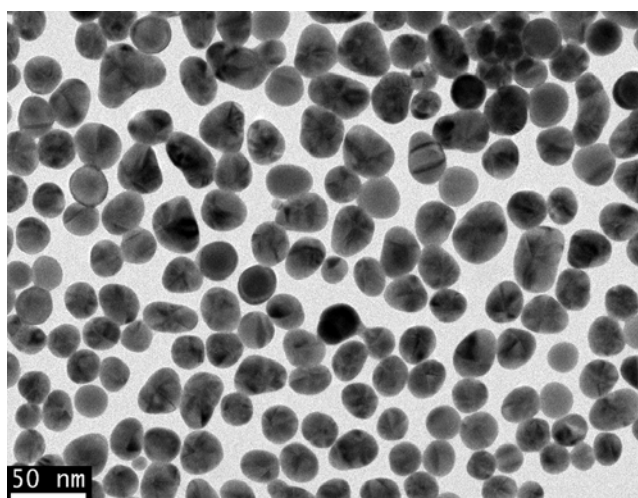


**Fig. S2.** TEM image of Au nanoparticles prepared in the absence of CTAB under otherwise identical synthetic conditions.

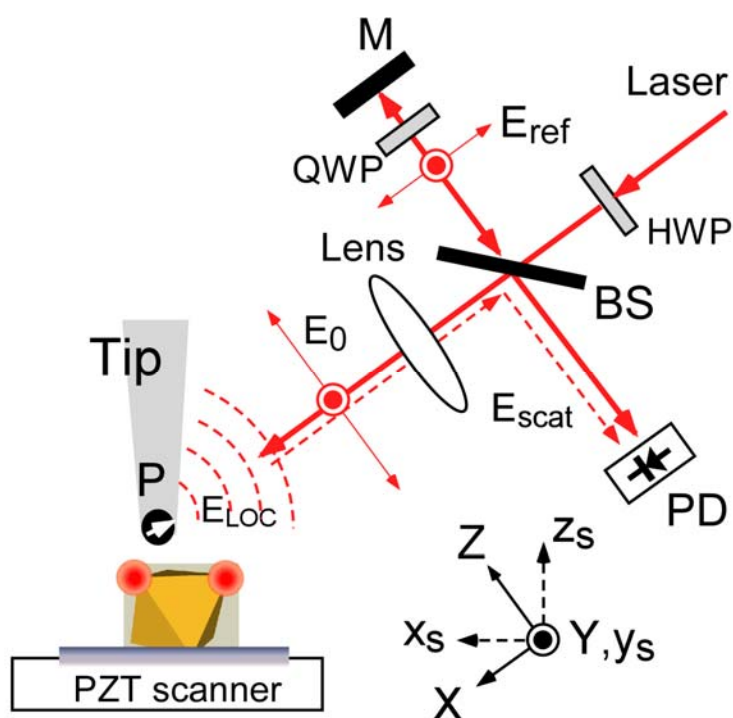


**Fig. S3.** The schematic setup of ANSOM: M = mirror, BS = 50/50 beam splitter, PD = photodiode, QWP = quarter-wave plate, HWP = half-wave plate,  $E_0$  = incident field and its polarization,  $E_{\text{ref}}$  = reference field and its polarization,  $E_{\text{scat}}$  = back-scattered field,  $E_{\text{LOC}}$  = localized field at the sample, and P = induced tip-dipole. The coordinate systems for the sample ( $x_s$ ,  $y_s$ ,  $z_s$ ) and the polarization (X, Y, Z) are rotated by  $30^\circ$  from each other. The (X,Z) and ( $x_s$ ,  $z_s$ ) are in the same plane.